Petrography, chemistry, and mineral compositions for subunits of the Tshirege Member, Bandelier Tuff within the Valles Caldera and Pajarito Plateau

Richard G. Warren, Fraser Goff, Emily C. Kluk, and James R. Budahn
2007, pp. 316-332. https://doi.org/10.56577/FFC-58.316

in:

Geology of the Jemez Region II, Kues, Barry S., Kelley, Shari A., Lueth, Virgil W.; [eds.], New Mexico Geological Society 58 th Annual Fall Field Conference Guidebook, 499 p. https://doi.org/10.56577/FFC-58

This page is intentionally left blank to maintain order of facing pages.

New Mexico Geological Society Guidebook, 58th Field Conference, Geology of the Jemez Mountains Region II, 2007, p. 316-332.

PETROGRAPHY, CHEMISTRY, AND MINERAL COMPOSITIONS FOR SUBUNITS OF THE TSHIREGE MEMBER, BANDELIER TUFF WITHIN THE VALLES CALDERA AND PAJARITO PLATEAU

RICHARD G. WARREN[1], FRASER GOFF[2], EMILY C. KLUK[3], AND JAMES R. BUDAHN[4]
[1]Comprehensive Volcanic Petrographics, 2622 H Rd., Grand Junction CO 81506, rgwcvp@ascol.net
[2]Department of Earth and Planetary Sciences, University of New Mexico, Albuquerque NM 87131
[3]Earth and Environmental Sciences Division, Los Alamos National Laboratory, Los Alamos NM 87545
[4]U.S.Geological Survey, Denver Federal Center MS 974, Box 25046, Denver, Colorado 80225

Abstract — The chemistry, petrography, and mineral compositions for subunits of the Tshirege Member, Bandelier Tuff, are well determined on the Pajarito Plateau within numerous publications by the Los Alamos National Laboratory. We summarize these characteristics to determine that these same subunits occur within the Valles caldera. Most trace oxides and a few major oxides determined by X-ray fluorescence and neutron activation individually discriminate among subunits, and taken together confidently discriminate among all except the uppermost two subunits. Such oxides are generally immobile, except for a few under the conditions of extensive, strong alteration within VC2A and VC2B (collectively VC2), holes drilled on the western side of the resurgent dome of the Valles caldera. Analytical errors may also obscure chemical correlations. Phenocrysts of quartz, immune to alteration, provide an effective petrographic discriminator between the uppermost two subunits. Feldspar phenocryst compositions by electron microprobe show maximum abundances of anorthoclase, equal to those of sanidine, near the middle of Smith and Bailey's (1966) uppermost subunit V of Tshirege Member; elsewhere within their subunit V sanidine strongly dominates over anorthoclase. Most subunits of the Tshirege Member as well as the underlying Otowi Member occur in VC2. VC2A bottoms within the Otowi Member, which directly overlies the Santa Fe Group within VC2B. Pre-Bandelier tuff, characterized from outcrop on the southwest margin of Valles caldera, does not occur within VC2B, undermining evidence for a precursor caldera to the Toledo caldera. The thicknesses and absences of particular subunits of the Tshirege Member within VC2 provide structural data that we explain by explosion and collapse of the Valles caldera rather than by subsequent postcaldera structural activity such as resurgence.

REGIONAL CHEMISTRY AND PETROGRAPHY OF THE TSHIREGE MEMBER

Virtually every well drilled to characterize groundwater beneath the Pajarito Plateau penetrates the Tshirege Member, which strongly dominates exposed rock within the canyons and mesa of the plateau (Rogers, 1995). Samples from these drill holes and nearby outcrop robustly define the geochemistry and petrography of the Tshirege, as well as underlying Cerro Toledo Formation and Otowi Member of the Bandelier Tuff, all formations within the Tewa Group (Bailey et al., 1969). Nearly all these chemical analyses and many petrographic analyses appear within reports by Los Alamos National Laboratory (LANL). In this paper, we add petrographic analyses for drill holes VC2A and VC2B (Appendix), and employ chemical and petrographic analyses for other locations within the Valles caldera (Goff et al., 2007). This body of work provides nearly 1000 sample splits with chemical analyses, and more than 200 splits with quantitative petrographic analyses for the Tewa Group from a region that covers a significant portion of the Jemez volcanic field (JVF; Smith et al., 1970). The area sampled for these analyses occupies a region about 30 km long and 12 km wide from the western edge of the Valles caldera to the eastern edge of the Pajarito Plateau (Fig. 1). The database described by Warren et al. (2005) includes all analysis from the Tewa Group used for this paper and cites each data source for each analysis.

SUBUNITS OF THE TSHIREGE MEMBER

We here describe geochemical characteristics that aid in the recognition of subunits within the Tshirege Member throughout the Pajarito Plateau and Valles caldera. Smith and Bailey (1966) first defined petrologic subunits I through V for the entire JVF and later workers defined lithologic subunits for the Pajarito Plateau that closely correspond to the original definitions (Broxton and Reneau, 1995). We divide the Tshirege into lower, middle, and upper parts (Fig. 2), applying definitions first described by Warren et al. (1997) on the westernmost Pajarito Plateau for middle and upper Tshirege, which divide subunit V of Smith and Bailey (1966). Rogers (1995) mapped our subunit 5 as subunit F, and our subunits 3t and 4 together as subunit E. Lewis et al. (2002) and Lavine et al. (2003) mapped subunit 3t, but mapped upper Tshirege as their subunit 4.

Subunits of the Tshirege at the Pajarito Plateau have been defined primarily based on lithology, alteration, and stratigraphic

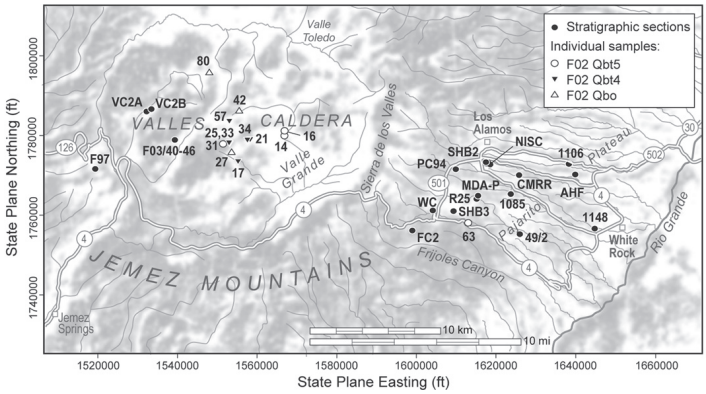

FIGURE 1. Locations of Tshirege Member of Bandelier Tuff used for laboratory analyses. For reference, F97 shows location of samples from San Diego Canyon Formation.

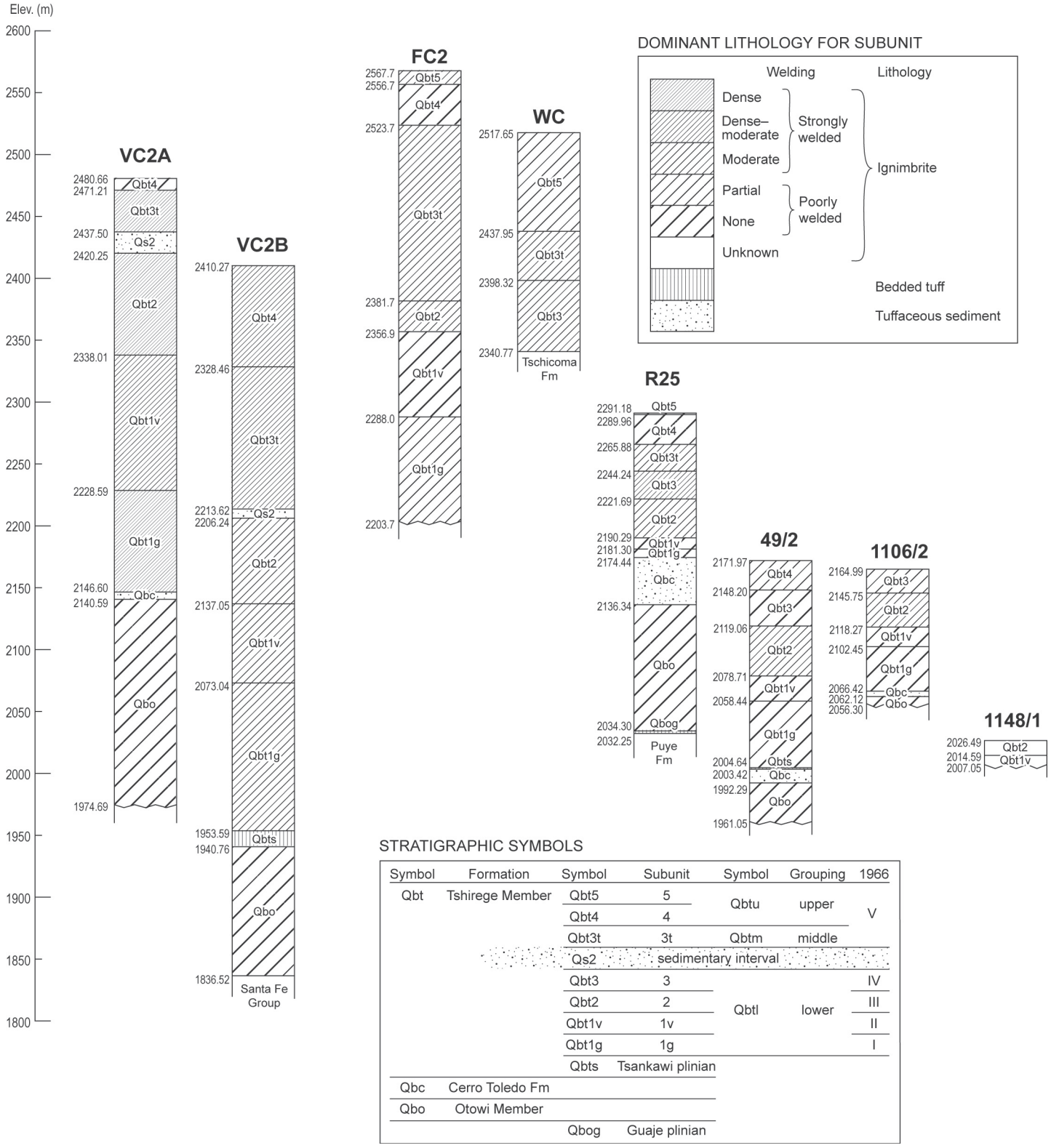

FIGURE 2. Stratigraphic columns for Tewa Group within Valles caldera and Pajarito Plateau. Locations are shown in Figure 1.

position, although Warren et al. (1997), Stimac et al. (2002), Lewis et al. (2002) and Lavine et al. (2003) have shown that subunits are also chemically distinct. Regional correlation based on lithology is unlikely to succeed, owing to generally striking lithologic differences between intracaldera and extracaldera tuff, as discussed by Smith and Bailey (1966) and as seen in Figure 2. The purpose of our paper is to evaluate whether the extensive body of geochemical and petrographic data used to help characterizes subunits of Tshirege on the plateau (Warren et al., 2005) can be accurately applied elsewhere within the JVF. Note that

we adopt names for subunits of the Tshirege defined by Broxton and Reneau (1995) because of their widespread usage, even though definitions are identical to definitions of Smith and Bailey (1966), and the subunit name "1g" is improperly descriptive for the lowest subunit. The letter "g" denotes "lower *glassy* tuff", for exposures of subunit Qbt1g within the Pajarito Plateau, but petrography demonstrates that the identical subunit was originally devitrified prior to hydrothermal alteration within the western Valles caldera in VC2.

CHEMISTRY OF THE TSHIREGE MEMBER

Typical samples

Stacks of histograms allow rapid visual comparison of oxide values among subunits of Tshirege Member (Fig. 3). Once we found the best visual fit of chemical and petrographic analyses based on subunit assignment, we assessed extreme alteration, analytical error, and abundance of lithic clasts as causes for outlying chemical values. For some samples, particularly those from VC2, alteration and abundance of lithic clasts had been determined from petrographic analyses. We assessed 3.2% of the 9048 oxide values for the Tewa Group as anomalous, as discussed below (see also Fig. 3) for several of the 17 oxides that we selected. These 17 oxides are the least susceptible to alteration, show the widest range of characteristic abundances within the Tshirege Member, and have generally excellent analytical accuracy, except as described below. With anomalous values eliminated, Table 1 presents average values for each oxide. Oxides compatible with primary minerals observed within the Tshirege Member (TiO_2, Fe_2O_3T, Sc_2O_3, SrO, BaO, and P_2O_5) increase in abundance upward within the unit, whereas incompatible oxides (Nb_2O_5, Y_2O_3, Yb_2O_3, ThO_2, UO_2, Rb_2O, and Cs_2O) decrease upward.

Each subunit of the Tshirege Member is chemically distinct from its stratigraphic neighbor, except for Qbt5 and Qbt4. Populations are single for most oxides and overlap within 1 sigma for neighboring subunits (Fig. 3; Table 1), but a suite of accurate analyses will invariably distinguish neighbors; subunit assignments are therefore highly amenable to multivariate analysis. Near its base, subunit Qbt4 shows a second population of more abundant compatible oxides associated with anorthoclase, as described below.

Comparing averages of three immobile oxides among locations of Figure 1 reveals a consistency of values among the widespread locations (Fig. 4). Only TiO_2 within Qbt3 reveals any significant progressive change, decreasing eastward from an average of 0.15% at MDA-P to 0.11% at AHF. Other compatible oxides also show a progressive eastward decrease for some subunits, and incompatible oxides tend to increase, but no such trends appear to be significant.

Lithic-rich samples and extreme alteration

A few samples (0.3% of analyses for Tewa Group) show anomalously high chemical values for most compatible oxides or for most incompatible oxides, usually without chemical or petrographic evidence of alteration. These samples are almost certainly a large lithic clast hidden behind a coating of adhering matrix, mistakenly sampled as representative, lithic-poor material. For example, petrographic analyses reveal that 4 of the 19 samples collected by Lewis et al. (2005) to characterize lithic-poor subunit Qbt3 contain 49% to 72% lithics. Anomalously high compatible oxides typically indicate a clast of dacite to andesite.

Samples from VC2 extremely challenge the application of chemical analyses for stratigraphic characterization. Intense argillic to propylitic alteration renders most alkalis and alkaline earth oxides useless for stratigraphic correlation within the entire column of VC2 (see Fig. 3). Nonetheless, alteration appears not to affect typically immobile oxides (Fig. 4), or even typically mobile oxides such as Cs_2O and UO_2 within specific portions of the Tshirege. This is surprisingly true even for Fe_2O_3T, which shows a distribution of values for each subunit indistinguishable from comparison values with unaltered samples in spite of extensive Fe mobilization as pyrite in VC2.

Analytical errors

Coauthors of this paper have produced 88% of the analyses for the Tewa Group applied in this paper, 80.3% by X-ray fluorescence (XRF) and 7.4% by neutron activation analysis (NAA). Oxides such as Fe_2O_3T, BaO, Rb_2O, and SrO reported for the same sample by each method invariably agree within uncertainties for accuracy provided for the XRF analyses within the database of Warren et al. (2005). Unfortunately, analytical quality is not as high for some published analyses that provide the only comparative chemical analyses for VC2. The extreme scatter for available comparative values of BaO (Fig. 5), is certainly due primarily to erroneously high BaO by XRF other than by our coauthors. Warren et al. (2003) found during their compilation of chemistry that analyses for Nb_2O_5 by other XRF are irreproducible; thus, all values for BaO and Nb_2O_5 by other XRF are excluded from averages. Values for Rb_2O show far less scatter, but indicate small but significant errors in other types of analyses. Note that analytical quality has been critically examined for all other oxides determined by other XRF and found to be good. Differences between averages for stratigraphically adjacent subunits of Tshirege Member are typically 10% to 20% of these averages, compared to analytical 2 sigma uncertainties that are typically 5% to 20% of the analytical value. Clearly, any significant error added to analytical uncertainty compromises the application of chemical analyses to define subunits of Tshirege Member.

PETROGRAPHY OF THE TSHIREGE MEMBER

Table 2 provides average contents of primary (phenocryst) minerals within each subunit of Tshirege Member. Alkali feldspar dominates within all subunits. Petrographic analyses (Figs. 4, 6) show significant differences in relative abundances of quartz between upper and middle Tshirege (Qbtum = Qbt5 through Qbt3t) and lower Tshirege (Qbtl = Qbt3 through Qbt1g), and in total phenocrysts between Qbtum and Qbtl. Phenocryst-poor samples occur only within Qbt1g at VC2 and at TA-21 (1106)

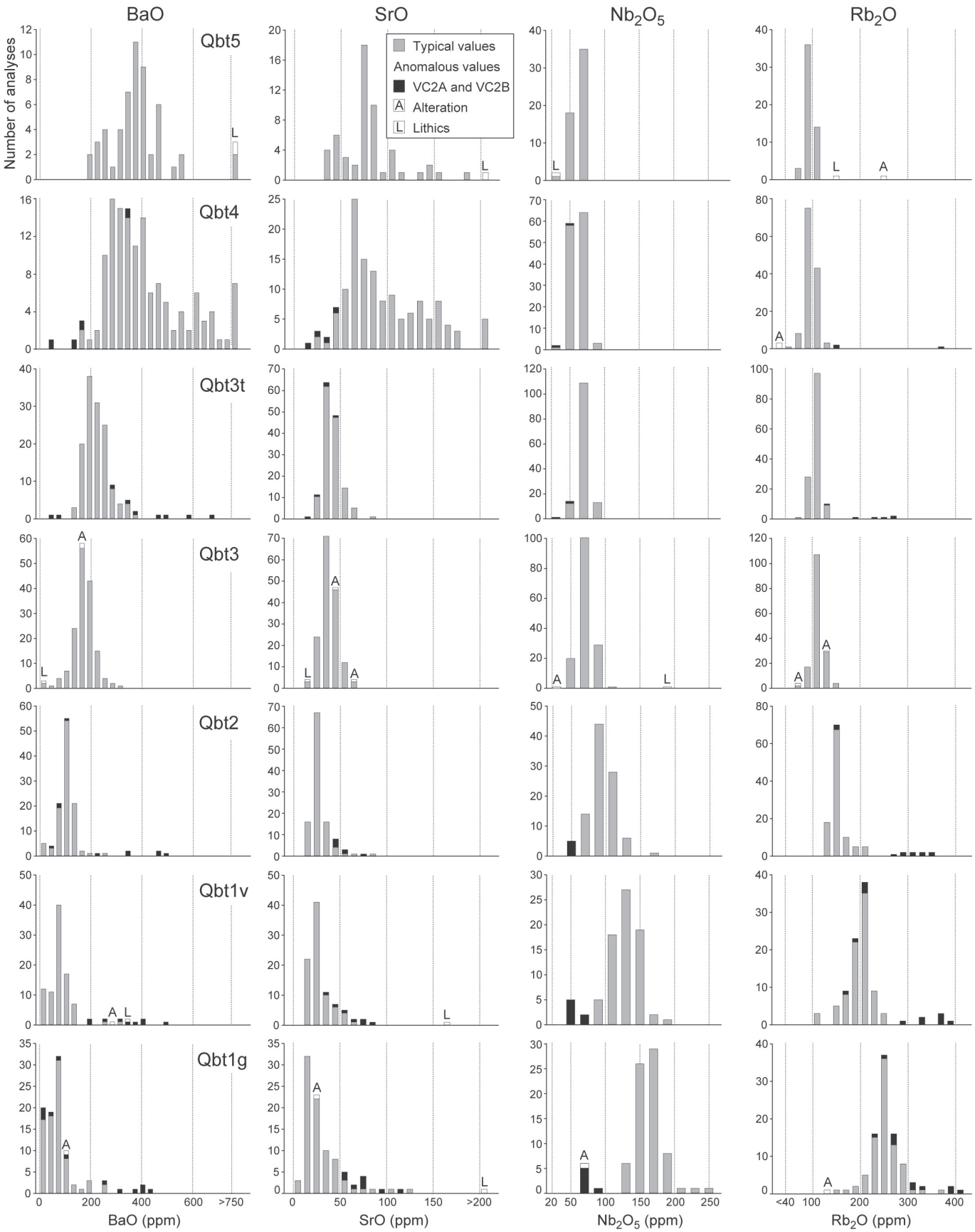

FIGURE 3. Histograms showing values of representative compatible oxides (BaO and SrO) and incompatible oxides (Rb_2O and Nb_2O_5) for subunits of Tshirege Member. We exclude anomalous values from averages.

TABLE 1. Averages of whole-rock chemistry for subunits of Tshirege Member. Separate averages are listed for anorthoclase-rich (*) and anorthoclase-poor Qbt4.

Strat	TiO_2 %			Fe_2O_3T %			Sc_2O_3 ppm			SrO ppm			BaO ppm			P_2O_5 %		
Unit	avg	2sig	n	avg	2sig	n	avg	2sig	n	avg	2sig	n	avg	2sig	n	avg	2sig	n
Qbt5	0.246	0.076	54	2.27	0.84	54				80	61	54	386	235	54	0.042	0.035	54
Qbt4	0.24	0.062	91	2.29	0.62	97	5.3	1.8	8	81	84	95	352	256	95	0.039	0.029	91
Qbt4*	0.378	0.154	39	2.93	1.00	39	4.3		1	150	90	38	605	298	38	0.074	0.055	38
Qbt3t	0.18	0.044	144	1.89	0.39	142	3.4	1.5	4	41	19	136	223	91	134	0.021	0.021	141
Qbt3	0.126	0.03	149	1.55	0.29	159	2.5	0.6	10	38	18	159	172	87	159	0.01	0.013	149
Qbt2	0.09	0.02	101	1.44	0.3	116	2	0.8	22	27	20	106	104	69	111	0.009	0.013	97
Qbt1v	0.08	0.017	79	1.47	0.26	95	1.8	0.7	17	27	21	84	81	83	83	0.008	0.014	73
Qbt1g	0.072	0.025	78	1.54	0.3	95	1.6	0.9	19	29	40	83	72	99	82	0.007	0.007	76

Strat	ZrO_2 ppm			HfO_2 ppm			La_2O_3 ppm			Ce_2O_3 ppm			Nb_2O_5 ppm			Y_2O_3 ppm		
Unit	avg	2sig	n	avg	2sig	n	avg	2sig	n	avg	2sig	n	avg	2sig	n	avg	2sig	n
Qbt5	484	85	54										62.1	16.6	54	46.1	31.8	54
Qbt4	452	81	96	10	2.1	8	82.4	54.6	10	143	24	8	63.3	19	88	45.6	22.3	88
Qbt4*	514	112	39	10.9		1	87.4		1	168		1	56	17	38	45.2	20.5	39
Qbt3t	426	85	141	9.5	2	4	70.7	22.8	6	140	27	4	70	16.4	134	47.7	14.9	137
Qbt3	313	59	159	8.2	1.5	10	63.7	11	10	131	31	10	71.1	21.2	149	47.3	17	149
Qbt2	281	54	116	9.1	1.2	22	63.8	9.8	22	132	17	22	96.4	33.2	93	66.2	31	96
Qbt1v	289	62	96	10.9	2	17	62.8	13.3	17	133	25	17	129.7	37.2	72	92.8	34	79
Qbt1g	316	87	95	12	2.7	14	61.8	11.4	19	132	25	19	164.1	40.8	72	119.7	33.2	76

Strat	Yb_2O_3 ppm			ThO_2 ppm			UO_2 ppm			Rb_2O ppm			Cs_2O ppm		
Unit	avg	2sig	n	avg	2sig	n	avg	2sig	n	avg	2sig	n	avg	2sig	n
Qbt5										95	21	53			
Qbt4	4.1	0.4	7	13.2	1.4	8	3.7	0.4	8	98	21	93	2	0.7	7
Qbt4*	5.7		1	17.8		1				89	24	37	1.9		1
Qbt3t	4.4	1.7	3	13.8	4.1	4	3.3		1	107	19	135	2.1	0.6	3
Qbt3	4.7	1.7	10	15.4	5.4	10	4.4	1.4	10	112	25	159	2.1	1.1	10
Qbt2	6.5	2	20	19.5	3.2	22	5.9	1.6	17	153	37	106	3.2	1.3	20
Qbt1v	9.1	2.1	17	26.2	4.9	17	8.5	1.6	17	197	50	85	5	1.3	13
Qbt1g	10.5	2.4	17	31.3	7.1	19	10.5	2.5	19	252	62	86	9.5	2.9	14

Average may exclude analyses as discussed in text. Values below detection limit are represented in average as half the detection limit (LLD). P_2O_5 analyses are strongly censured for lower Tshirege (Qbt3 and lower), with 11% below LLD for Qbt3t, 51% below LLD for Qbt3 and 79% below LLD for Qbt2. Very few analyses (generally <1%) fall below LLD for other elements.

locations (Fig. 2), solidifying the subunit correlation between these distant locations. The average content of quartz phenocrysts differs significantly (at 95% confidence) among individual units of Qbtum, providing the only petrographic or geochemical measure to distinguish subunit Qbt5. Mafic phenocrysts are primarily clinopyroxene, and associated (Fe-rich) olivine important within subunit Qbt2 and below, and associated orthopyroxene important within subunit Qbt3 and above. Mafics are typically strongly altered to pseudomorphic forms, a few preserving pyroxene relicts except within fairly uncommon vitric ignimbrite.

The database of Warren et al. (2005) demonstrates that the lower Tshirege Member is petrographically indistinguishable from the Otowi Member except for a significantly higher lithic content of the Otowi, and the database also types the San Diego Canyon Formation as highly quartz- and phenocryst-poor compared to Bandelier Tuff. These petrographic data, compared with our analyses for VC2 (Appendix) demonstrate that the Bandelier Tuff is the sole volcanic unit within VC2 (Fig. 2), in sharp contrast to the original lithologic logs (Hulen et al., 1988; Hulen and Gardner, 1989).

Petrographic analyses provide insightful information to assess sample alteration and lithic abundances, which affect chemical values, as described above. For example, sample VC2A-1601.6 is highly quartz- and phenocryst-poor, and certainly represents an inadvertently sampled lithic of underlying San Diego Canyon Formation within the Otowi Member. Particularly in concert with X-ray diffraction analyses, petrographic analyses define the nature of alteration, guiding insightful assessment of the chemical mobility. Except in sample VC2B-1447.2, feldspar phenocrysts throughout VC2 have been destroyed, replaced mostly by the secondary feldspars albite and adularia (see Warren et al., 2005; Fig. 7). Given that adularia is highly K-rich, enrichment of whole-rock K_2O and Rb_2O is expected and observed in VC2 (Fig. 3).

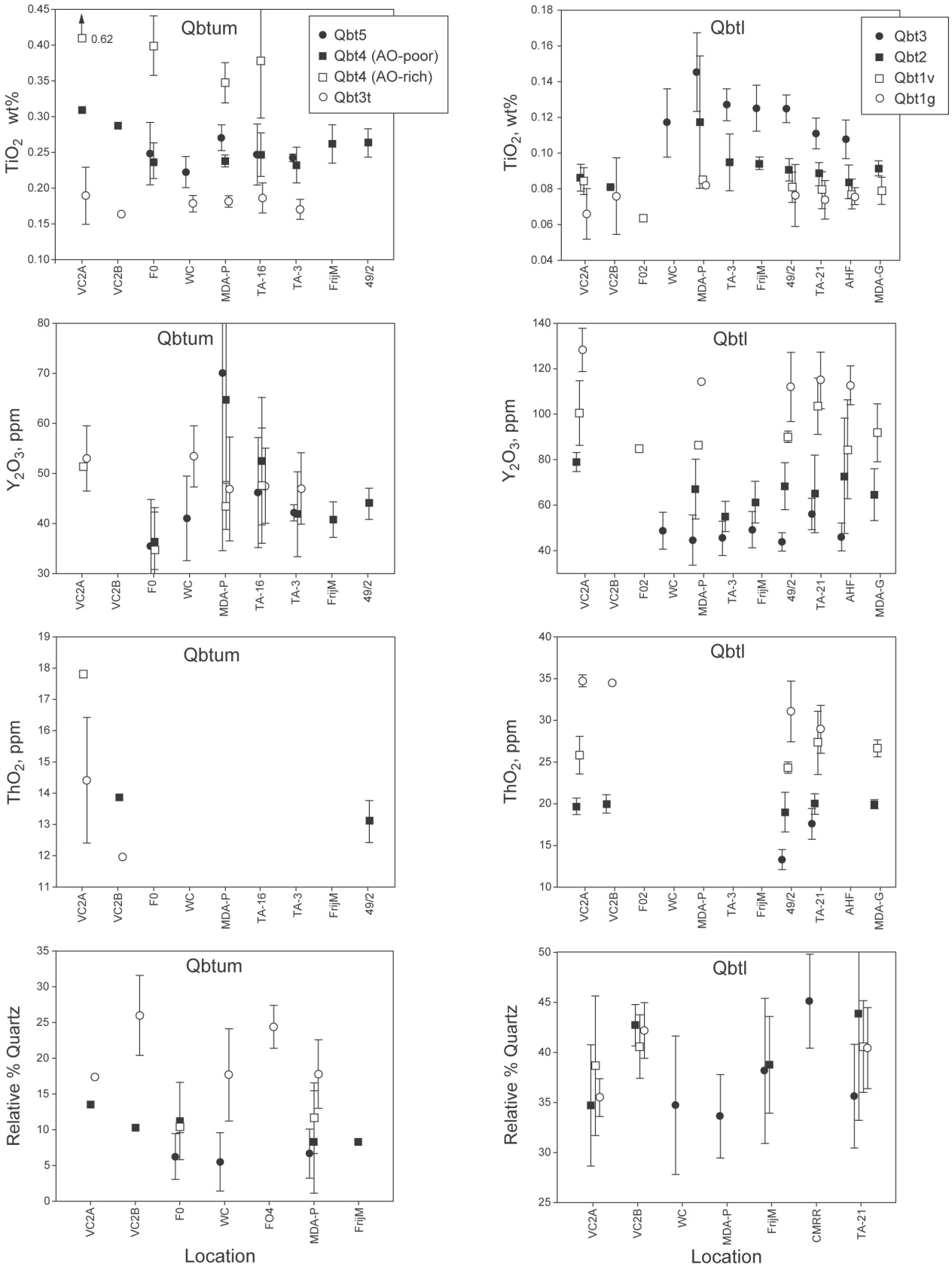

FIGURE 4. Averages and one sigma for compatible oxide TiO_2 and incompatible oxides Y_2O_3 and ThO_2 for subunits of the Tshirege Member at stratigraphic sections shown in Figures 1 and 2. We exclude anomalous values from averages. Bottom diagrams show averages and one sigma for quartz as a percentage of phenocrysts.

TABLE 2. Averages of primary mineral abundances for subunits of Tshirege Member. Separate averages are listed for anorthoclase-rich (*) and anorthoclase-poor Qbt4, and for phenocryst-poor (*) and phenocryst-rich Qbt1g.

Strat Unit	K-spar (KF)			Quartz (QZ)			Plagioclase (PL)			Mafics (MA)			Orthopx (OX)			Clinopx (CX)		
	avg	2sig	n	avg	2sig	n	avg	2sig	n	avg	2sig	n	avg	2sig	n	avg	2sig	n
Qbt5	86.47	9.2	17	6.08	6.78	17	1.42	4.84	17	3.63	4.96	17	0.76	1.74	12	1.37	2.89	12
Qbt4	83.23	10.62	10	11.17	8.51	11	1.59	2.74	10	2.76	4.57	10	0.48	0.94	6	1.98	2.67	6
Qbt4*	80.46	18.9	7	8.94	11.92	7	6.54	6.89	7	2.63	2.73	7	1.4	1.21	5	1.62	1.48	5
Qbt3t	74.89	14.99	20	20.84	12.88	22	0.63	2.34	20	2.9	5.55	22	0.44	1.33	12	1.54	2.36	12
Qbt3	59.65	14.22	58	38.43	14.24	58	0.32	0.86	58	1.1	1.23	58	0.03	0.17	50	0.89	1.23	52
Qbt2	57.6	14.59	24	40.23	14.59	24	0.38	0.67	24	1.35	1.86	24	0	0.01	17	0.74	1.35	18
Qbt1v	58.87	10.58	14	39.5	11.4	16	0.52	1.54	14	0.97	1.92	16	0	0	4	0.95	1.23	4
Qbt1g*	63.69	14.21	4	31.82	14.33	4	0.9	2.4	4	2.7	5.54	4	0	0	3	1.69	0.84	3
Qbt1g	58.16	8.93	14	39.84	8.04	16	0.49	0.99	14	1.12	2.2	16	0	0	6	0.96	0.69	6
TPd	61.46	54.76	2	1.92	0.51	2	31.87	40.85	2	7.15		1	4.26		1	2.89		1

Strat Unit	Olivine (OL)			Biotite (BT)			Hornblnd (HN)			Fe-Ti oxid (FX)			Magnetite (MT)			Ilmenite (IL)		
	avg	2sig	n	avg	2sig	n	avg	2sig	n	avg	2sig	n	avg	2sig	n	avg	2sig	n
Qbt5	0.01	0.05	16	0	0	17	0	0.01	17	1.8	3.62	17	1.55	3.13	17	0.24	1.15	17
Qbt4	0	0.01	9	0.02	0.09	10	0.01	0.02	9	1.53	1.81	11	1.44	1.87	10	0.04	0.15	9
Qbt4*	0	0	5	0	0.01	7	0.01	0.04	7	1.25	1.21	7	1.13	1.09	7	0.13	0.2	7
Qbt3t	0.08	0.62	14	0.05	0.5	22	0.02	0.07	19	1.11	2.69	22	1.1	2.69	22	0	0.01	22
Qbt3	0.02	0.18	54	0	0.02	58	0.07	0.19	58	0.5	0.68	58	0.53	0.85	29	0	0	29
Qbt2	0.27	0.73	18	0.04	0.2	24	0.19	0.41	23	0.44	0.76	24	0.52	1.45	6	0	0	6
Qbt1v	0.23	0.34	4	0.02	0.12	16	0.05	0.19	16	0.22	0.88	16	0.21	1.02	12	0	0	12
Qbt1g*	0	0	3	0	0	4	1.43	4.87	4	0.89	1.98	4						
Qbt1g	0.28	1.1	8	0.02	0.13	16	0.05	0.19	16	0.34	0.86	16	0.3	1.07	10	0	0	10
TPd	0		1	0		1	0		1	3.04	2.61	2	2.73	3.49	2	0.62		1

Strat Unit	Perri/Chev (PE)			Apatite (AP)			Zircon (ZR)			Phenocrysts (PH)			Lithics (LI)			Normzd Phenos		
	avg	2sig	n	avg	2sig	n	avg	2sig	n	avg	2sig	n	avg	2sig	n	avg	2sig	n
Qbt5	0.003	0.003	5	0.119	0.081	5	0.062	0.066	5	20.51	11.97	17	0.46	0.89	17	26.17	14.3	17
Qbt4	0.027	0.043	4	0.05	0.08	5	0.096	0.162	5	20.31	16.52	11	1.38	1.8	11	25.84	15.08	11
Qbt4*	0.007	0.008	6	0.143	0.131	6	0.058	0.041	6	19.67	8.49	7	3.94	6.52	7	30.38	7.11	7
Qbt3t	0.022	0.029	7	0.03	0.033	7	0.038	0.028	7	19.19	9.03	22	1.04	2.85	22	24.94	11.35	22
Qbt3	0.016	0.02	4	0.008	0.015	4	0.015	0.009	4	24.41	9.48	58	1.65	4.61	58	38.09	13.01	58
Qbt2	0.014		1	0.006		1	0.004		1	24.23	9.36	24	1.35	4.52	24	31.29	10.86	24
Qbt1v										21.91	11.65	16	2.22	7.37	16	31.82	12.95	16
Qbt1g*										4.22	4.9	4	0.37	0.34	4	7.35	7.79	4
Qbt1g										22.54	12.86	16	1.62	3.86	16	32.72	13.43	16
TPd	0		1	0.171		1	0.038		1	3.6	6.62	2	2.78	1.64	2	6.07	11.18	2

Except for final 3 abundances, averages are percent of total phenocrysts (PH). Final 3 columns are volume percent of sample; final column is corrected first to 0% lithics, and then to 0% porosity based on assumed porosities by lithology: vitrophyre (0%), densely welded tuff (10%), moderately welded tuff (20%), partially welded tuff (30%), nonwelded tuff (40%), bedded tuff (50%). Averages include only values with a QA level of 1 from Warren et al. (2005) for QZ, KF, PE, AP, and ZR. Averages for all other components include QA level 2 for LI where QA level of 1 is unavailable.

CHEMISTRY OF K-SPAR PHENOCRYSTS WITHIN THE TSHIREGE MEMBER

Alkali feldspar becomes increasingly sodic and calcic upward within the Tshirege Member (Caress, 1995). The compositional trends within sanidine are slight; the most important feature is appearance of prominent anorthoclase (Fig. 6) within subunit Qbt4. The four samples DEB/5/95 from MDA-P (Fig. 1) are stacked in stratigraphic sequence, showing that anorthoclase is prominent within the lower to middle part of subunit Qbt4 (Warren et al., 1997). Sample DEB/5/95/6, originally assigned as subunit Qbt4t, is transitional in chemistry and petrography between subunits Qbt4 and Qbt3t. Samples with prominent anorthoclase have relatively high contents of plagioclase, invariably thickly armored with anorthoclase, and elevated compatible oxide contents. In the absence of microprobe analyses, we assume that the second population for subunit Qbt4 with strongly elevated compatible oxides reflects a population with an abundance of anorthoclase, termed subunit Qbt4 (AO-rich). Within this subunit, anorthoclase and sanidine abundances are similar; no samples are known or suspected from exhaustive petrographic analyses to contain anorthoclase strongly dominant over sanidine. We find that our upper/

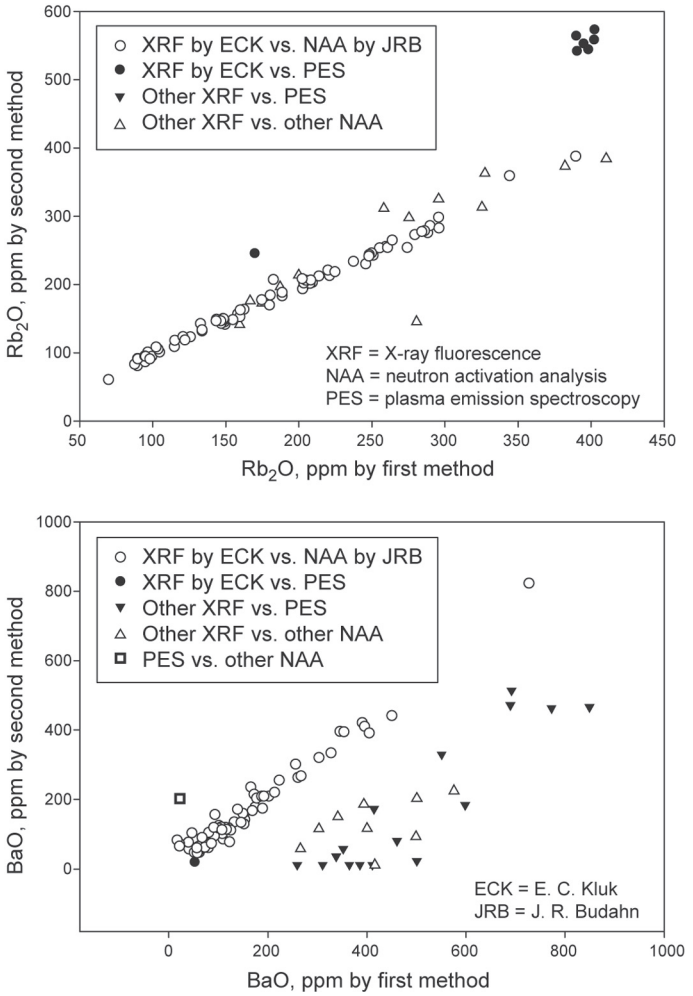

FIGURE 5. Plots of analyses for selected oxides determined within the same sample by different analysts and/or methods.

middle Tshirege Member, although stratigraphically equivalent, does not petrographically match subunit V, described by Smith and Bailey (1966) as exclusively containing anorthoclase.

THICKNESSES FOR SUBUNITS OF THE TSHIREGE MEMBER

The lowest subunits of the lower Tshirege are thickest within VC2 and at the FC2 section within Frijoles Canyon of the Pajarito Plateau (Figs. 2, 8). If the similar thicknesses for Qbt1g and Qbt1v at these well-separated locations reflect equal distance from the source, then these subunits erupted from the southeastern part of the Valles caldera, where the Tshirege is thickest (Nielson and Hulen, 1984). Additionally, subunits of lower Tshirege are thickest within southernmost locations of the Pajarito Plateau, indicating a generally lower topography in that direction prior to eruption of the Tshirege.

Qbt3 is presently recognized only within the Pajarito Plateau. The subunit is not presently recognized within the Valles caldera or within Frijoles Canyon (Figs. 2, 8), suggesting a source localized near the northeastern part of the Valles caldera. This suggestion is supported by lateral variations in both compatible and incompatible oxides described earlier.

Thick accumulations of sediment, 17.25 m of debris flow deposits in VC2A (Hulen et al., 1988) and 7.38 m of probably fluvial deposits in VC2B (Hulen and Gardner, 1989), interpose between subunits Qbt3t and Qbt2 (Fig. 2). This sediment indicates that a significant time gap followed eruption of subunit Qbt2 before eruption of middle Tshirege Member (Qbt3t), and/or caldera collapse during the same time period. Favoring the notion of a significant time gap between middle and lower Tshirege Member is a noticeably different total phenocryst content (Fig. 6; Table 2) and zirconium content (Table 1) between the two units. Although time gaps between subunits of Tshirege are suspected from other evidence (Broxton and Reneau, 1995), such direct evidence is heretofore unrecognized.

Markedly thicker upper and middle Tshirege Member (Qbt3t and Qbt4) in VC2B (196.65 m) compared to VC2A (43.16 m) may also be related to an episode of caldera collapse prior to or concurrent with eruption of the middle and/or upper Tshirege. If this were true, ground level at VC2B would have been structurally lower than levels at VC2A immediately prior to eruption of Qbt3t. Alternatively, this difference in thickness may simply reflect later faulting associated with the intense hydrothermal activity found within these two wells.

Qbt5 is absent in VC2; its westernmost documented occurrence is 33 m thick within stratigraphic section F03/40-46 along the Redondo Border, as described in Goff et al. (2007). It is unknown north of Los Alamos Canyon (Figs. 2, 8). This suggests a source for Qbt5 localized near the southeastern part of the Valles caldera, possibly blocked from deposition at VC2 by the emerging Redondo Peak dome (Goff et al., 2007). Like most uppermost, mafic-rich subunits of voluminous regional ignimbrites (see data in Warren et al., 2003), Qbt5 extends a short distance from its source in the caldera.

VARIATIONS IN CHARACTER AND THICKNESS FOR SUBUNITS OF THE TSHIREGE MEMBER

Subunits of the Tshirege Member within the Pajarito Plateau, defined on the basis of field characteristics, have been mapped throughout the plateau, aided by accurate and sensitive chemical and petrographic analyses. In this paper, we summarize these petrologic characteristics for subunits and correlate them with samples within the Valles caldera, most importantly with the stratigraphic columns of VC2 in westernmost locations within the caldera.

Distributions of each subunit suggest that most of them erupted from the eastern side of the Valles caldera rather from a central source. Subunit Qbt3 is presently unknown within the caldera, and probably erupted from the eastern side of the Valles caldera, where it lies unidentified beneath sedimentary deposits. Each subunit shows progressively decreasing abundances for compatible oxides and increasing abundances for incompatible oxides eastward from the western end of the Pajarito Plateau, although the trend is significant only for TiO_2 in Qbt3. A loss of heavy primary minerals such as magnetite during transport of the ignim-

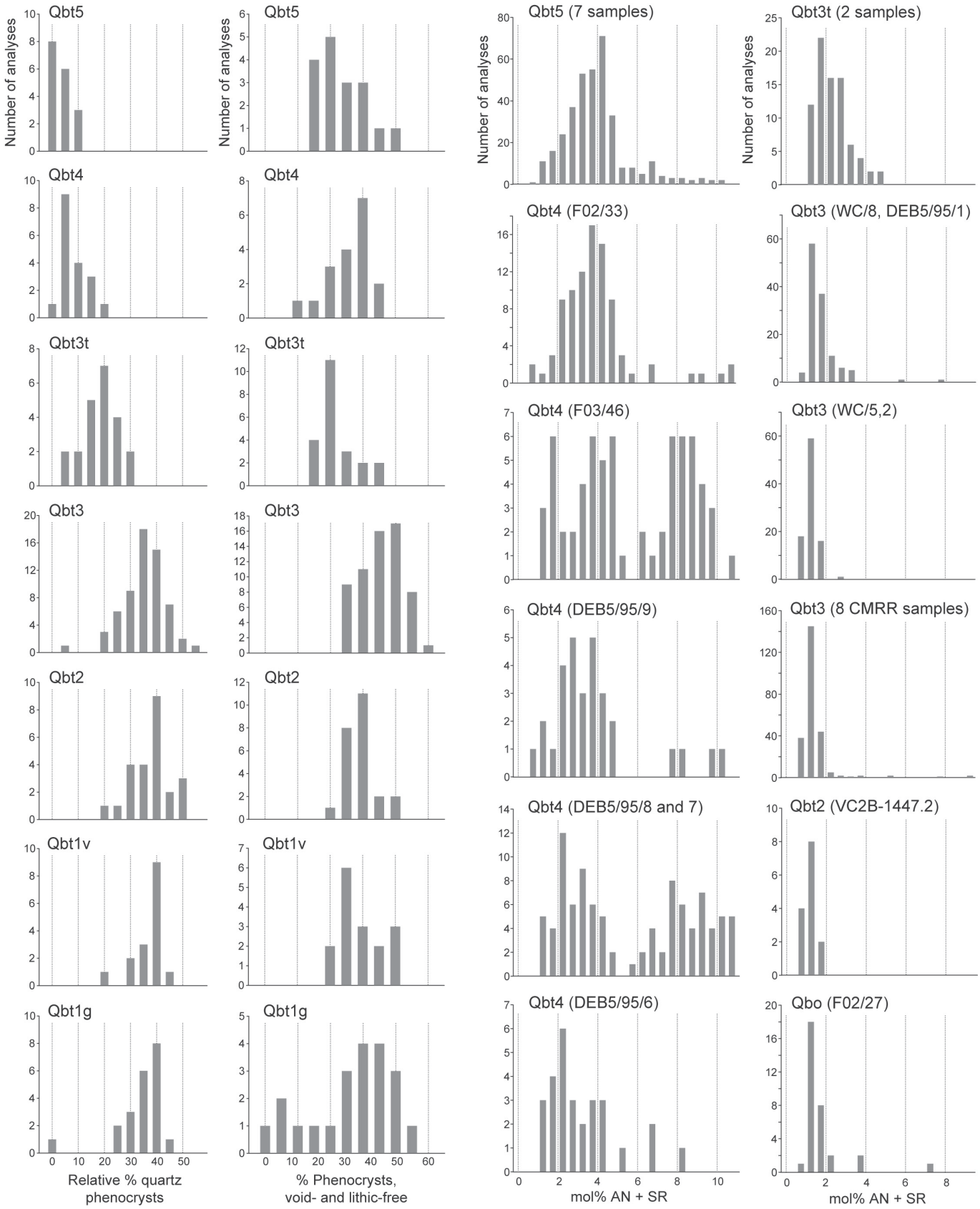

FIGURE 6. Histograms to left show quartz as a percentage of phenocrysts for subunits of the Tshirege Member and total phenocrysts, corrected for lithics and for estimated porosity. Estimated porosities for tuff are 0% for vitrophyre, 10% for densely welded, 20% for moderately welded, 30% for partially welded, 40% for nonwelded, 50% for bedded. Histograms to right show anorthite plus strontian (AN+SR) mol% content of alkali feldspar for subunits of the Tshirege Member.

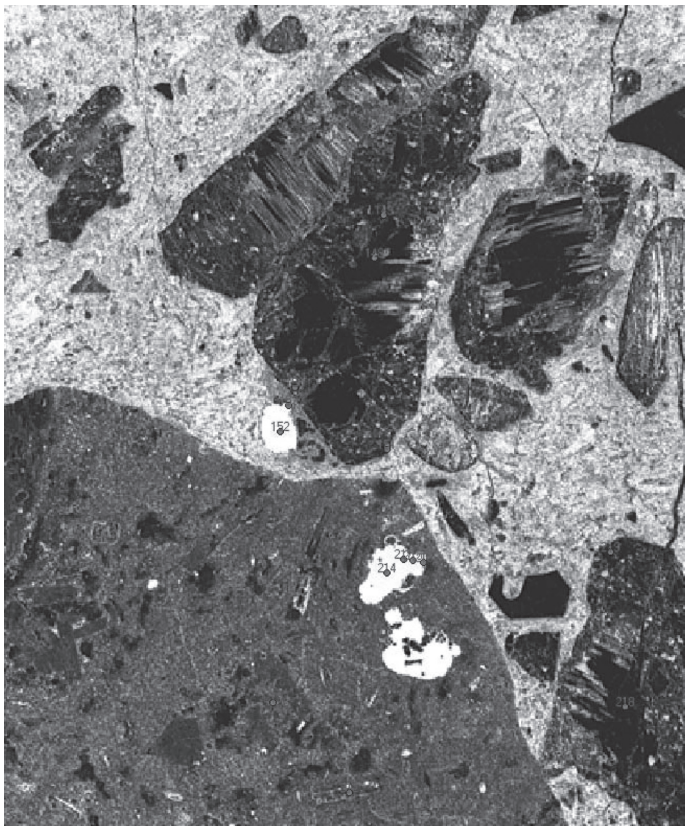

FIGURE 7. Points utilized for petrographic and mineral chemical analysis of split VC2B-1447.2(C. Negative image in transmitted light shows felsic phenocrysts as dark features; quartz, unaltered, is uniformly black, and alkali feldspar has streaked appearance caused by partial alteration to adularia and albite. Point 152 is magnetite partly altered to pyrite, and point 214 is an oxidized intergrowth of magnetite and ilmenite. The large feature in lower left third of image is a single lithic of intermediate composition lava. This split provides the sole thin section from VC2 that retains any primary alkali feldspar.

brite away from an easterly source is consistent with the chemical trends.

Prominent anorthoclase, plagioclase armored by anorthoclase, and markedly higher abundances of compatible oxides occur within the upper/middle Tshirege Member, first described by Warren et al. (1997) as reverse zoning. This certainly represents an injection of relatively primitive magma into the Tshirege magma system. Hornblende is virtually absent in this primitive magma, which therefore differs from primitive magma injected into the lower Tshirege (Stimac, 1996).

The San Diego Canyon Formation, a quartz- and crystal-poor unit recognized within its namesake canyon as a pair of ignimbrites, is absent within VC2. Petrographic analyses nullify its presence in both VC2A and VC2B, calling into question its identification in the subsurface of the Valles caldera (Nielson and Hulen, 1984).

Up to 17 m of sediment interposes between subunits Qbt3t and Qbt2 in VC2, providing direct evidence for a significant time gap, possibly tens of years, between the middle and lower Tshirege Member. This sedimentary layer is probably widespread in the subsurface of the Valles caldera, where upper and middle Tshirege may have been misidentified as "Upper Tuff" (Nielson and Hulen, 1984), as in it was in VC2A. Markedly thicker upper and middle Tshirege Member in VC2B compared to VC2A may be a structural feature related to a late episode of caldera collapse concurrent with eruption of middle and/or upper Tshirege.

ACKNOWLEDGMENTS

Dave Broxton, Dave Vaniman, and Jamie Gardner and his team were prominent among many geologists of LANL who sampled stratigraphic sections throughout the Pajarito Plateau. The fruits of their labor are the sets of samples providing the analyses serving as the basis for this paper. The vast majority of these analyses, credited in the database of Warren et al. (2005) but too numerous to cite in this paper are published in LANL reports. We thank Dave Broxton and Greg Cole for providing thoughtful reviews and Andi Kron for graphics support.

REFERENCES

Bailey, R.A., Smith, R.L., and Ross, C.S., 1969, Stratigraphic nomenclature of volcanic rocks in the Jemez Mountains, New Mexico: U.S. Geological Survey, Bulletin 1274-P, 19 p.

Broxton, D.E., and Reneau, S.L., 1995, Stratigraphic nomenclature of the Bandelier Tuff for the Environmental Restoration Project at Los Alamos National Laboratory, Los Alamos, New Mexico: Los Alamos National Laboratory, Report LA-13010-MS, 21 p.

Caress, M.E., 1995, Alkali feldspars in the Tshirege Member of the Bandelier Tuff: systematic and lateral distribution of feldspar compositions and their implications [Ph.D. dissertation]: Santa Barabara, University of California, 151 p.

Goff, F., Warren, R.G., Goff, C.J., Whiteis, J., Kluk, E., and Counce, D., 2007, Comments on the geology, petrography, and chemistry of rocks within the resurgent dome, Valles caldera, New Mexico: New Mexico Geological Society, 58th Field Conference, Guidebook, p. 354-366.

Hulen, J.B., and Gardner, J.N., 1989, Field geologic log for Continental Scientific Drilling Program core hole VC-2B, Valles caldera, New Mexico DOE/ER/13196-4 (ESL-89025-TR): Earth Science Laboratory, University of Utah Research Institute, Salt Lake City UT, 92 p.

Hulen, J.B., Gardner, J.N., Nielson, D.L., and Goff, F., 1988, Stratigraphy, structure, hydrothermal alteration and ore mineralization encountered in CSDP corehole VC-2A, Sulphur Springs area, Valles caldera, New Mexico: a detailed overview, DOE/ER/13555-1 (ESL-88001-TR): Earth Science Laboratory, University of Utah Research Institute, Salt Lake City UT, 55 p.

Lavine, A., Lewis, C.J., Katcher, D.K., Gardner, J.N., and Wilson, J., 2003, Geology of the north-central to northeastern portion of Los Alamos National Laboratory, New Mexico: Los Alamos National Laboratory, Report LA-14043-MS, 44 p.

Lewis, C J., Lavine, A., Reneau, S.L., Gardner, J.N., Channell, R., and Criswell, C.W., 2002, Geology of the western part of Los Alamos National Laboratory (TA-3 to TA-16), Rio Grande rift, New Mexico: Los Alamos National Laboratory, Report LA-13960-MS, 98 p.

Lewis, C.J., Warren, R.G., Gardner, J.N., Chipera, S., and Lavine, A., 2005, Petrographic and geochemical analyses of Bandelier Tuff unit Qbt3 from boreholes at the Chemistry and Materials Research Replacement site and nearby outcrops, Los Alamos National Laboratory, New Mexico: Los Alamos National Laboratory, Unlimited Release LA-UR-95-3841, 64 p.

Nielson, D.L., and Hulen, J.B., 1984, Internal geology and evolution of the Redondo Dome, Valles caldera, New Mexico, Journal of Geophysical Research, v. 89, p. 8695-8712.

Rogers, M.A., 1995, Geologic map of Los Alamos National Laboratory reservation: State of New Mexico Environmental Department, scale 1:4800.

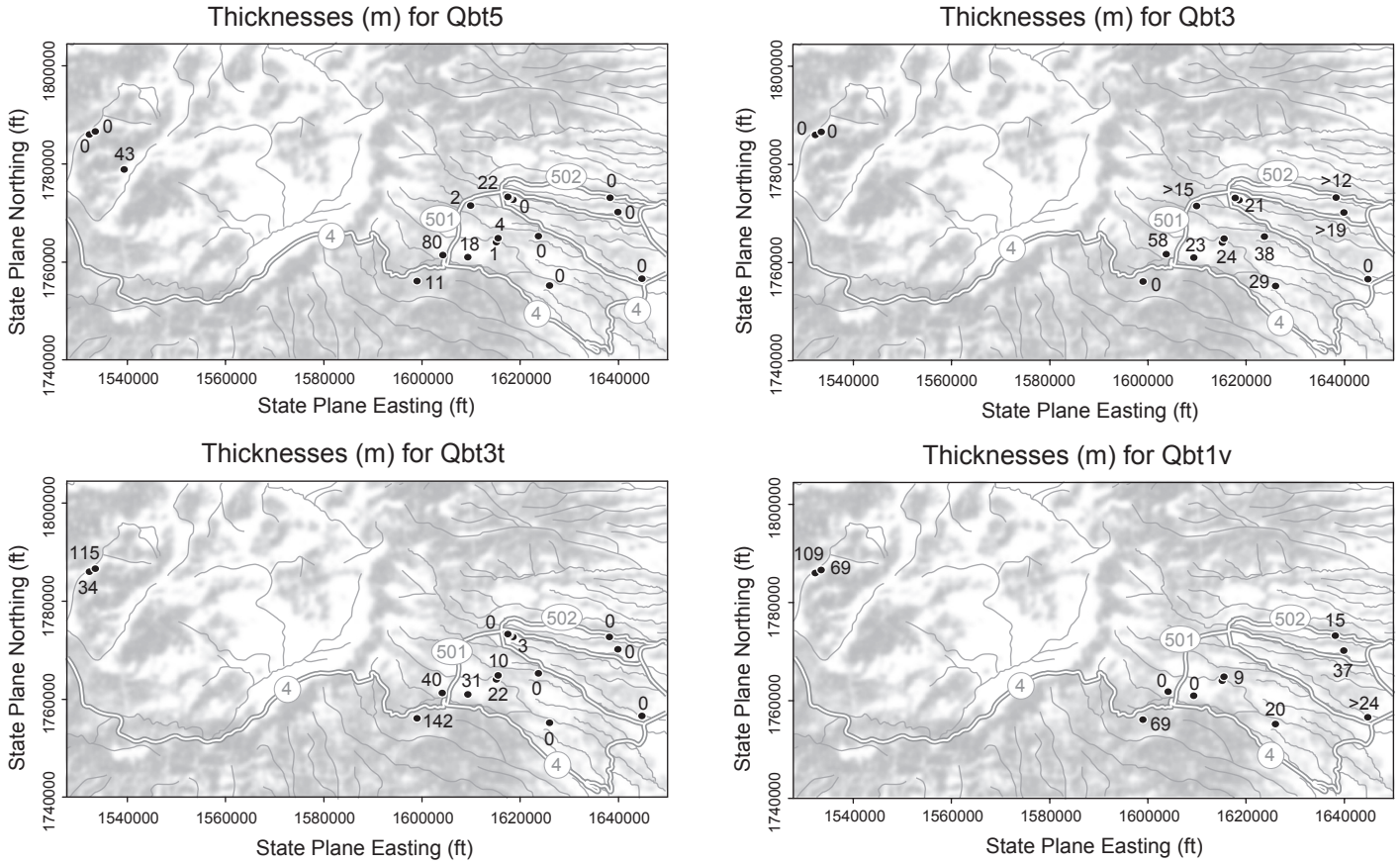

FIGURE 8. Thicknesses in meters for selected subunits of the Tshirege Member. Stratigraphic sections located in Figure 1 and displayed in Figure 2.

Smith, R.L., and Bailey, R.A., 1966, The Bandelier Tuff: a study of ash-flow eruption cycles from zoned magma chambers: Bulletin Volcanologique, v. 29, p. 83-103.

Smith, R.L., Bailey, R.A., and Ross, C.S. 1970, Geologic map of the Jemez Mountains, New Mexico: U.S. Geological Survey, Miscellaneous Geological Investigations Map I-571, scale 1:125 000.

Stimac, J.A., 1996, Hornblende-dacite pumice in the Tshirege Member of the Bandelier Tuff: implications for magma chamber and eruptive processes: New Mexico Geological Society, 47th Field Conference, Guidebook, p. 269-283.

Stimac, J.A., Broxton, D.E., Kluk, E.C., Chipera, S.J., and Budahn, J.R., 2002, Stratigraphy of the tuffs from borehole 49-2-700-1 at Technical Area 49, Los Alamos National Laboratory, New Mexico: Los Alamos National Laboratory, Report LA-13969, 14 p.

Warren, R.G., Cole, G.L., Broxton, D.E., Kluk, E.C., Chipera, S.J., WoldeGabriel, G., Vaniman, D.T., Snow, M.G., and Goff, F., 2005, A database of geochemical, petrographic, mineralogic, and geochronological analyses for the Jemez volcanic field to support the 3-D geologic model of the Pajarito Plateau, Los Alamos National Laboratory, New Mexico: Los Alamos National Laboratory, Unlimited Release LA-UR-05-2976.

Warren, R.G., McDonald, E.V., and Ryti, R.T., 1997, Baseline geochemistry of soil and bedrock Tshirege Member of the Bandelier Tuff at MDA-P: Los Alamos National Laboratory, Report LA-13330-MS, 89 p.

Warren, R.G., Sawyer, D.A., Byers, F.M. Jr., and Cole, G.L., 2003, A petrographic, geochemical, and geophysical database and stratigraphic framework for the southwestern Nevada volcanic field: Los Alamos National Laboratory, Unlimited Release LA-UR-03-1503, 54 p.

APPENDIX. Petrographic analyses by R.G. Warren for polished thin sections from VC2.

Comp	Unit	Abun	Alt	Meth	Comp	Unit	Abun	Alt	Meth	Comp	Unit	Abun	Alt	Meth
VC2A-95.8(D Qbt4 NWT														
LI	T	11.3		1	QZ	T	2.36		1					
VC2A-99(A Qbt4 NWT														
AP	P	45.3	U	L	LI	T	2.14		1	VO	T	9.61		1
FE	T	12.8	M	1	PY	P	3560	X	1	ZR	P	88.3	U	C
FS	T	11	F	1	QZ	T	1.78	U	1					
VC2A-151(C Qbt3t MWT														
AP	P	80.6	U	C	MN	P	2.64	U	C	QZ	T	3.94	U	2
BT	P	17.8	Z	A	OL	P	0		A	SN	P	0		A
FE	T	20.4	M	1	PE	P	96.3	F	L	VO	T	3.56		1
KF	T	15.9	F	1	PL	T	0.324	F	1	VQ	T	0.647	X	1
LI	T	0.656		2	PY	P	22700	X	1	ZR	P	121	U	C
VC2A-212.5(C Qbt3t DWT														
LI	T	1.9		1	QZ	T	1.27		1					
VC2A-292.8(C Qbt2 DWT														
LI	T	1.15		1	QZ	T	10.8		1					
VC2A-297(A Qbt2 DWT														
FE	T	28.7	M	1	PY	P	2000	X	Q	VE	T	10.2	X	1
KF	T	20.4	F	1	QZ	T	8.36	U	1	VO	T	3.64		1
LI	T	0.364		1										
VC2A-352.7(D Qbt2 DWT														
LI	T	0		1	QZ	T	10.7		1					
VC2A-407(B Qbt2 MWT														
FE	T	21.1	M	1	PY	P	11200	X	1	PY	P	11200	X	1
KF	T	13.6	F	1	QZ	T	7.48	U	1	QZ	T	7.48	U	1
LI	T	1.12		1										
VC2A-500.5(B Qbt2 MWT														
FE	T	17.6	M	1	PY	P	1000	X	Q	VE	T	0.2	X	1
KF	T	10	F	1	QZ	T	7.6	U	1	VO	T	4.2		1
LI	T	10.6		1										
VC2A-553(D Qbt1v MWT														
FE	T	19.6	M	1	VO	T	6.21		1	QZ	T	9.66	U	1
KF	T	10.8	F	1	FE	T	22.3	M	1	VE	T	0.63	X	1
PY	P	12000	X	1	KF	T	12.6	F	1	VO	T	6.72		1
QZ	T	8.82	U	1	PY	P	10500	X	1					
VC2A-600(C Qbt1v MWT														
FE	T	26.1	M	1	PY	P	1500	X	Q	VE	T	2.11	X	1
KF	T	14.9	F	1	QZ	T	11.2	U	1	VO	T	1.68		1
LI	T	1.89		1										
VC2A-653.3(C Qbt1v DWT														
CC	T	0.671	X	1	LI	T	2.01		1	QZ	T	9.73	U	1
FE	T	26.2	M	1	PL	T	0.336	F	1	VE	T	0.336	X	1
FL	P	500	X	Q	PY	P	1000	X	Q	VO	T	1.01		1
KF	T	16.4	F	1										
VC2A-709(A Qbt1v NWT														
CC	T	28.8	X	1	PY	P	4080	X	1	SL	P	50	X	Q
FE	T	12.9	M	1	QD	T	4.29	X	1	VE	T	40.6		1
FS	T	7.96	F	1	QZ	T	4.9	U	1	VO	T	0		1
LI	T	0.612		1										
VC2A-713(C Qbt1v NWT														
FE	T	23.7	M	1	LI	T	0.811		1	QZ	T	9.94	U	1
KF	T	13.8	F	1	PY	P	1000	X	Q	VO	T	7.1		1

APPENDIX (continued). Petrographic analyses by R.G. Warren for polished thin sections from VC2.

Comp	Unit	Abun	Alt	Meth	Comp	Unit	Abun	Alt	Meth	Comp	Unit	Abun	Alt	Meth
VC2A-752(C Qbt1v NWT														
CC	T	0.94	X	1	LI	T	8.46		1	VE	T	0.564	X	1
FE	T	22.2	M	1	PY	P	1880	X	1	VO	T	1.13		1
KF	T	12	F	1	QZ	T	10.2	U	1					
VC2A-807(C Qbt1v NWT														
CC	T	0.397	X	1	LI	T	1.39		1	QZ	T	3.97	U	1
FE	T	16.3	M	1	PL	T	0.397	F	1	VE	T	4.37	X	1
FL	P	1980	X	1	PY	P	1500	X	Q	VO	T	1.19		1
KF	T	11.9	F	1										
VC2A-857(C Qbt1v NWT														
CC	T	0.743	X	1	LI	T	2.23		1	QZ	T	8.18	U	1
FE	T	24.9	M	1	PL	T	0.372	F	1	VO	T	8.92		1
KF	T	16.4	F	1	PY	P	3720	X	1					
VC2A-904.4(C Qbt1g MWT														
FE	T	25	M	1	LI	T	1.86		1	QZ	T	9.5	U	1
FL	P	2070	X	1	PL	T	0.207	F	1	VO	T	1.65		1
KF	T	15.3	F	1	PY	P	1500	X	Q					
VC2A-954.4(C Qbt1g NWT														
CC	T	1.81	X	1	LI	T	0.202		1	QZ	T	8.06	U	1
FE	T	23.6	M	1	PY	P	1000	X	Q	VO	T	4.23		1
KF	T	15.5	F	1										
VC2A-999.8(C Qbt1g MWT														
CC	T	0.215	X	1	LI	T	0.43		1	QZ	T	8.39	U	1
FE	T	24.5	M	1	PY	P	2150	X	1	VO	T	2.8		1
KF	T	16.1	F	1										
VC2A-1051.8(C Qbt1g NWT														
CC	T	0.03	X	Q	FL	P	978	X	1	PY	P	500	X	Q
CH	T	0.293	X	1	KF	T	5.08	F	1	QZ	T	1.96	U	1
FE	T	7.04	M	1	LI	T	0.489		1	VO	T	0.587		1
VC2A-1108(C Qbt1g DWT														
LI	T	0.477		1	QZ	T	10		1					
VC2A-1150(B Qbt1g MWT														
CC	T	0.319	X	1	KF	T	16.9	F	1	QZ	T	11.5	U	2
FE	T	30.7	M	1	LI	T	0.281		2	VO	T	0		1
FL	P	2500	X	Q	PY	P	300	X	Q					
VC2A-1201(C Qbo DWT														
LI	T	5.22		1	QZ	T	4.96		1					
VC2A-1254(C Qbo NWT														
CC	T	0.342	X	1	LI	T	0.342		1	QZ	T	7.53	U	1
FE	T	18.8	M	1	PY	P	6850	X	1	VO	T	7.19		1
KF	T	11.3	F	1										
VC2A-1302(C Qbo PWT														
CC	T	1.2	X	1	LI	T	1.81		1	QZ	T	7.23	U	1
FE	T	22.1	M	1	PY	P	16100	X	1	VO	T	6.02		1
KF	T	14.9	F	1										
VC2A-1357(C Qbo NWT														
FE	T	21.8	M	1	LI	T	6.36		1	QZ	T	7.71	U	1
KF	T	14.1	F	1	PY	P	3850	X	1	VO	T	9.25		1
VC2A-1408(C Qbo NWT														
CC	T	1.29	X	1	LI	T	42.4		1	QZ	T	6.8	U	1
FE	T	14.9	M	1	PL	T	0.647	F	1	VO	T	3.24		1
KF	T	7.44	F	1	PY	P	2000	X	Q					

APPENDIX (continued). Petrographic analyses by R.G. Warren for polished thin sections from VC2.

Comp	Unit	Abun	Alt	Meth	Comp	Unit	Abun	Alt	Meth	Comp	Unit	Abun	Alt	Meth
VC2A-1443(B Qbo NWT														
CC	T	1.31	X	1	LI	T	87.9		1	QZ	T	1.87	U	1
FE	T	3.73	M	1	PL	T	0.187	F	1	VO	T	0.746		1
KF	T	1.68	F	1	PY	P	250	X	Q					
VC2A-1510(C Qbo NWT														
CC	T	5.33	X	1	LI	T	31		1	QZ	T	5.67	U	1
FE	T	12	M	1	PL	T	1	F	1	VO	T	2.67		1
KF	T	5.33	F	1	PY	P	6670	X	1					
VC2A-1553(B Qbo NWT														
LI	T	12.5		1	KF	T	6.29	F	1	PY	P	1000	X	Q
QZ	T	7.08		1	LI	T	12.6		1	QZ	T	5.5	U	1
CC	T	1.96	X	1	PL	T	0.393	F	1	VO	T	3.54		1
FE	T	12.2	M	1										
VC2A-1601.6(C TPd NWT (lithic fragment)														
AP	G	1	U	M	LI	T	2.2		L	PY	P	2000	X	Q
FE	T	1.26	M	L	MT	P	500	F	Q	QZ	T	0.022	U	L
FX	P	500	F	Q	PL	T	0.22	F	L	ZR	G	2	U	M
KF	T	1.02	F	L										
VC2A-1652(B Qbo NWT														
LI	T	17.3		1	QZ	T	4.15		1					
VC2A-1701(C Qbo NWT														
CC	T	0.418	X	1	KF	T	11.9	F	1	QZ	T	7.11	U	1
FE	T	19	M	1	LI	T	1.88		1	VO	T	1.05		1
FL	P	2090	X	1	PY	P	6280	X	1					
VC2A-1730.5(C Qbo NWT														
CC	T	2.39	X	1	LI	T	12.6		1	QZ	T	5.8	U	1
FE	T	15	M	1	PL	T	0.683	F	1	VO	T	1.02		1
KF	T	8.53	F	1	PY	P	1000	X	Q					
VC2B-602(A Qbt4 NWT														
LI	T	8.28		1	QZ	T	6.42		1					
VC2B-650(A Qbt4 MWT														
LI	T	2.1		1	QZ	T	2.33		1					
VC2B-701.7(C Qbt4 MWT														
LI	T	6.6		1	QZ	T	4		1					
VC2B-749.5(A Qbt4 DWT														
LI	T	4.57		1	QZ	T	2.05		1					
VC2B-800.8(A Qbt4 MWT														
FE	T	12	M	1	PY	P	3320	X	1	VE	T	5.65		1
KF	T	10.6	F	1	QZ	T	1.33	U	1	VO	T	3.99		1
LI	T	1.33		1										
VC2B-849.4(A Qbt3t MWT														
FE	T	16.4	M	1	MC	T	0.207	U	1	VE	T	0.83		1
FE	T	16.4	M	1	PY	P	6220	X	1	VO	T	3.94		1
FE	T	16.4	M	1	QZ	T	4.56	U	1					
VC2B-899.1(C Qbt3t DWT														
FE	T	14.5	M	1	PY	P	6900	X	1	VE	T	2.07		1
KF	T	9.31	F	1	QZ	T	5.17	U	1	VO	T	1.72		1
LI	T	0.345		1										
VC2B-950.4(A Qbt3t MWT														
FE	T	15.7	M	1	PL	T	0.419	F	1	QZ	T	3.14	U	1
KF	T	12.2	F	1	PY	P	12600	X	1	VO	T	1.05		1
LI	T	4.61		1										

APPENDIX (continued). Petrographic analyses by R.G. Warren for polished thin sections from VC2.

Comp	Unit	Abun	Alt	Meth	Comp	Unit	Abun	Alt	Meth	Comp	Unit	Abun	Alt	Meth
VC2B-999.5(A	**Qbt3t**	**NWT**												
FE	T	11.5	M	1	MC	T	0.192		1	QZ	T	2.88	U	1
FS	T	8.65	F	1	PY	P	1000	X	Q	VO	T	7.69		1
LI	T	4.04		1										
VC2B-1050.5(A	**Qbt3t**	**DWT**												
LI	T	4		1	QZ	T	2.67		1					
VC2B-1101.5(A	**Qbt3t**	**NWT**												
CH	T	0.183	X	1	LI	T	1.1		1	QZ	T	3.66	U	1
FE	T	13.9	M	1	PY	P	1830	X	1	VO	T	11.9		1
KF	T	10.2	F	1										
VC2B-1149.6(A	**Qbt3t**	**NWT**												
FE	T	21.5	M	1	LI	T	3.13		1	VE	T	0.347		1
FE	T	21.5	M	1	QZ	T	4.86	U	1	VO	T	6.94		1
VC2B-1194(A	**Qbt3t**	**MWT**												
FE	T	19	M	1	LI	T	2.74		1	QZ	T	6.2	U	1
FS	T	12.8	F	1	PY	P	5470	X	1	VO	T	2.19		1
VC2B-1249.5(C	**Qbt2**	**DWT**												
LI	T	0.295		1	QZ	T	15.9		1					
VC2B-1303.2(A	**Qbt2**	**MWT**												
FE	T	34.9	M	1	LI	T	0.346		1	VO	T	1.04		1
KF	T	19	F	1	QZ	T	15.9	U	1					
VC2B-1399.5(A	**Qbt2**	**MWT**												
CC	T	0.187	X	1	LI	T	0.375		1	VE	T	0.187	X	1
FE	T	27.7	M	1	QZ	T	11.2	U	1	VO	T	1.12		1
KF	T	16.5	F	1										
VC2B-1447.2(C	**Qbt2**	**MWT**												
AL	P	0		A	GX	T	0.318	F	1	PE	P	48.2	Z	A
AP	P	21.3	U	L	HN	P	0		A	PL	T	0.0234	F	1
BT	P	34.7	U	E	IL	P	3.81	F	E	PY	P	200	X	Q
CC	T	0.3	X	Q	KF	T	18.8	Z	1	QZ	T	14.3	U	1
CX	P	1070	F	E	LI	T	4.14		1	SN	P	0		A
FE	T	33.1	M	1	MA	P	1680	M	E	VE	T	0.637		1
FL	P	100	X	Q	MN	P	0		A	VO	T	0.637		1
FX	P	1000	M	E	MT	P	1000	Z	E	ZR	P	13.2	U	C
GT	P	0		A	OY	P	572	F	E					
VC2B-1500(A	**Qbt1v**	**MWT**												
FE	T	29.5	M	1	LI	T	0.996		1	VE	T	0.598	X	1
KF	T	18.5	F	1	QZ	T	11	U	1	VO	T	1.59		1
VC2B-1556(A	**Qbt1v**	**MWT**												
FE	T	32.7	M	1	KF	T	18.6	F	1	QZ	T	14.2	U	1
FL	P	2580	X	1	LI	T	0.773		1	VO	T	0.515		1
VC2B-1599.5(A	**Qbt1v**	**MWT**												
CC	T	0.203	X	1	LI	T	0.203		1	VE	T	0.811		1
FE	T	25.8	M	1	QZ	T	11	U	1	VO	T	0.609		1
FS	T	14.8	F	1										
VC2B-1649(A	**Qbt1v**	**NWT**												
LI	T	1.96		1	QZ	T	15.1		1					
VC2B-1704(A	**Qbt1g**	**MWT**												
FE	T	30.4	M	1	LI	T	6.98		1	QZ	T	11.5	U	1
KF	T	18.7	F	1	PL	T	0.205	F	1	VO	T	1.23		1

APPENDIX (continued). Petrographic analyses by R.G. Warren for polished thin sections from VC2.

Comp	Unit	Abun	Alt	Meth	Comp	Unit	Abun	Alt	Meth	Comp	Unit	Abun	Alt	Meth
VC2B-1752(C Qbt1g MWT														
CC	T	0.355	X	2	FS	T	17	F	2	QZ	T	12.9	U	2
FE	T	29.9	M	2	LI	T	0.71		2	VO	T	1.18		2
VC2B-1799.5(A Qbt1g MWT														
CC	T	0.591	X	1	LI	T	1.38		1	VE	T	1.77		1
FE	T	28	M	1	PY	P	200	X	Q	VO	T	2.17		1
FS	T	15.4	F	1	QZ	T	12.6	U	1					
VC2B-1851(A Qbt1g NWT														
CC	T	0.368	X	1	KF	T	13.4	F	1	QZ	T	11.4	U	1
CH	T	0.735	X	1	PL	T	0.184	F	1	VO	T	9.01		1
FE	T	25	M	1	PY	P	1000	X	Q					
VC2B-1900.4(A Qbt1g MWT														
FE	T	27.5	M	1	LI	T	0.537		1	QZ	T	12	U	1
KF	T	15.6	F	1	PY	P	1790	X	1	VO	T	2.33		1
VC2B-1949.5(A Qbt1g DWT														
LI	T	2.91		1	QZ	T	9.22		1					
VC2B-2001.5(C Qbt1g MWT														
FE	T	20.6	M	1	PL	T	0.327	F	1	QZ	T	8.5	U	1
KF	T	11.8	F	1	PY	P	3270	X	1	VO	T	3.59		1
LI	T	5.56		1										
VC2B-2050(A Qbts BED														
LI	T	13		1	QZ	T	19.4		1					
VC2B-2099.5(A Qbo NWT														
CC	T	1.03	X	1	KF	T	8.44	F	1	PY	P	0.8	X	Q
FE	T	17.1	M	1	LI	T	16.7		1	QZ	T	8.23	U	1
FL	P	100	X	Q	PL	T	0.412	F	1	VO	T	6.79		1
VC2B-2145(A Qbo NWT														
CC	T	1.94	X	1	LI	T	14.2		1	QZ	T	7.74	U	1
FE	T	21.9	M	1	PL	T	0.645	F	1	VO	T	7.1		1
KF	T	13.5	F	1										
VC2B-2199.6(C Qbo NWT														
LI	T	17.8		1	QZ	T	7.38		1					
VC2B-2252.7(A Qbo NWT														
CC	T	0.402	X	1	LI	T	27.3		1	QZ	T	3.41	U	1
FE	T	9.04	M	1	PL	T	1	F	1	VO	T	3.61		1
KF	T	4.62	F	1										
VC2B-2300(A Qbo NWT														
CC	T	1.26	X	1	LI	T	20.9		1	QZ	T	6.69	U	1
FE	T	15.3	M	1	PL	T	1.05	F	1	VO	T	5.65		1
KF	T	7.53	F	1	PY	P	1.7	X	Q					
VC2B-2353(A Qbo NWT														
CC	T	0.337	X	1	LI	T	22.2		1	QZ	T	6.4	U	1
FE	T	14.8	M	1	PL	T	0.337	F	1	VO	T	0.673		1
KF	T	8.08	F	1										
VC2B-2402.9(A Qbo DWT														
LI	T	12.4		1	QZ	T	8.07		1					

Components: allanite (AL), apatite (AP), biotite (BT), calcite (CC), chlorite (CH), clinopyroxene (CX), felsic phenocrysts (FE), fluorite (FL), feldspar phenocrysts (FS), Fe-Ti oxides (FX), garnet (GT), groundmass K-spar (GK), groundmass Fe-Ti oxides (GX), hornblende (HN), ilmenite (IL), K-spar phenocrysts (KF), lithics (LI), mafic phenocrysts (MA), microcline (MC), monazite (MN), magnetite (MT), olivine (OL), orthopyroxene (OX), olivine or pyroxene (OY), perrierite/chevkinite (PE), total phenocrysts (PH), plagioclase phenocrysts (PL), pyrite (PY), drusy quartz (QD), quartz phenocrysts (QZ), sphalerite (SL), sphene (SN), vein (VE), void >30 microns (VO), vein quartz (VQ), zircon (ZR).

Units of measure: grains (G), parts per million by volume (P), percent by volume (T).

Abundances: Values are those with a QA level of 1 from Warren et al. (2005); values of lower QA level are excluded.

Component alteration: unaltered (U), almost entirely altered (Z), pseudomorphic (F), mixed, individual members of mineral group have different alteration (M), secondary (X).
Analysis method (see Warren, et al., 2003 for detailed descriptions): single point count (1), two point counts (2), all areas (A), exhaustive grain count (C), extrapolation (E), estimated from largest grains (L), count of conspicuous grains (M), estimate (Q).
Stratigraphic unit: See Figure 2, also San Diego Canyon formation (TPd).
Lithology (all tuff): bedded (BED), nonwelded (NWT), partially welded (PWT), moderately welded (MWT), densely welded (DWT).
Sample type: all core, VC2A-1601.6 is lithic from core.